Original Article

Effect of sintering temperature on mechanical properties and ion release of fluorohydroxyapatite (FHA)-filled dental resin composites

Maryam Hezarjaribi[1,2], Majid Akbari[2,3], Seyyedeh Fatemeh Namdar[2,3], Arash Esmaili[4], Zeinab Foroughi[4], Fatemeh Mollaei[4], Ebrahim Farah[4], Arsalan Shahri[4], Hossein Bagheri[1,2]

Abstract

Objective: Smart ion-releasing restorative materials may increase the success and survival rate of composite dental restorations. This study aimed to evaluate the impact of sintering temperature on the mechanical properties and ion-releasing behavior of fluorohydroxyapatite (FHA)-filled dental resin composites.

Methods: The FHA was synthesized via a sol-gel method and sintered at three temperatures (250, 500, and 1000ºC). FHA fillers were characterized using X-ray diffraction (XRD) and Fourier Transform Infrared (FTIR) spectroscopy, then coated with citric acid and incorporated (40% w/w) into a photo-curable resin matrix (Bis-GMA, TEGDMA, HEMA; weight ratio 2:1:1). Flexural strength (FS) and diametral tensile strength (DTS) were measured, as well as the depth of cure, which was determined by the Vickers microhardness test. The release of calcium and fluoride ions was monitored for a month in diluted citric acid (pH=4.3), and the effect of acidic storage on mechanical properties was evaluated via DTS testing. The filler distribution was observed via scanning electron microscopy. The influence of sintering temperature on the measured variables was statistically analyzed using one-way and two-way ANOVA (α=0.05).

Results: The XRD results revealed increased crystallinity with higher sintering temperatures. Correspondingly, mechanical properties improved with increasing sintering temperature ($P<0.05$), whereas the depth of cure, as well as ion release (Ca^{+2} and F^-), decreased ($P<0.05$).

Conclusions: Sintering at elevated temperatures yielded a greater amount of crystalline apatite structure, and enhanced mechanical properties of FHA-filled dental resin composites, but reduced ion release. Based on these findings, FHA fillers sintered at approximately 500ºC appear optimal for creating smart dental resin composite. *(J Dent Mater Tech 2023;12(2):(82-90)*

Keywords: Fluoride, Fluorohydroxyapatite, Resin composite, Sintering, Tensile strength

Introduction

The past several decades have witnessed remarkable advancements in dental composite technology, which coupled with rising aesthetic demands, have made resin composite restorations an increasingly popular choice for tooth restoration (1). Despite this progress, recent meta-analyses suggest that the long-term success of these restorations is often compromised by recurrent caries (2, 3).

One approach to this challenge involves smart or stimuli-responsive materials that can adapt to changes in their environment such as pH variations (4). Calcium phosphates, specifically calcium apatites, demonstrate this feature through phase transformations and ion release (5-7). Given their chemical and physical resemblance to dental tissue structures, calcium apatites have been explored as potential filler phases in dental composites and adhesives (8-14). Notably, these apatites are capable of releasing ions in acidic (cariogenic) conditions, potentially fostering self-mineralization under supersaturated conditions (12, 14, 15). Recent studies have highlighted synthetic fluorine-doped calcium hydroxyapatite bioceramics

[1]Dental Materials Research Center, Mashhad University of Medical Sciences, Mashhad, Iran
[2]Department of Restorative Dentistry, School of Dentistry, Mashhad University of Medical Sciences, Mashhad, Iran
[3]Dental Research Center, Mashhad University of Medical Sciences, Mashhad, Iran
[4]Student Research Committee, School of Dentistry, Mashhad University of Medical Sciences, Mashhad, Iran

Corresponding Author: Hossein Bagheri
Dental Materials Research Center, Mashhad University of Medical Sciences, Mashhad, Iran

Email: Bagherih@mums.ac.ir

Accepted: 28 May 2023. Submitted: 1 January 2022.

DOI: 10.22038/JDMT.2023.62327.1498

(fluorohydroxyapatite or FHA) as promising remineralizing agents. The incorporation of fluoride ions, well-known to enhance the remineralization process, allows FHA to actively contribute to the repair of artificial enamel lesions (16-20).

It is important to note that the sol-gel synthesis process of apatite structures, especially the calcination temperature, can significantly influence the crystallite size and overall crystallinity (21, 22). Higher crystallinity percentages have been linked with improved mechanical and physical properties and altered solubility, ultimately affecting the bioactivity of apatite bioceramics (22).

Considering the potential impact of fillers on the properties of dental resin composites, the current study aimed to evaluate the influence of different calcination temperatures on the physical and mechanical properties, as well as the bioactivity of an experimental FHA-filled dental resin composite. Through this investigation, we sought to determine an optimal calcination temperature for creating a bioactive dental composite.

Materials and Methods

Preparation and characterization of ceramic filler particles

The synthesis of fluorohydroxyapatite (FHA) was based on a sol-gel method. We used a solution of ammonium dihydrogen phosphate ((NH4) H2PO4) (Merck, Darmstadt, Germany) and infused it with sodium fluoride to achieve a P/F molar ratio of 6. This mixture was added dropwise into a calcium nitrate tetrahydrate solution under vigorous stirring to establish final concentrations of 0.3M for Ca^{2+}, 0.18M for $PO4^{3-}$, and 0.03M for F^{-}. The pH of the solution (10-11) was controlled using a pH electrode (WTW SenTix 97T probe) and adjusted with a 1 M sodium hydroxide solution when necessary. After aging the precipitated gel at room temperature overnight, the powder was produced via centrifugation, followed by three times washing with deionized distilled water and air-drying. The powder was finally calcined at three distinct temperatures (250, 500, and 1000°C) in an electrical furnace for 30 min, with a heating rate of 10°/min.

We examined the produced ceramic using X-ray diffraction (XRD) and Fourier Transform Infrared (FTIR) spectroscopy to characterize its crystalline structure. The XRD (X' Pert PW 3040/60, Philips, Netherlands) assessment allowed us to determine the mean crystallite size and the fraction of the crystalline phase, as previously described (22). For estimating the mean crystalline size, the line-broadening measurement of (211) line was used in Scherrer's equation (eq. 1):

$$D = \frac{0.89\lambda}{\beta Cos\theta} \quad \text{(eq. 1)}$$

In this equation, λ is the wavelength (CuKα), β is the full width at half-maximum of the fluorine hydroxyapatite (211) line, and θ is the diffraction angle

The X_c of the FHA powders was estimated using the following equation (eq. 2):

$$B_{002}\sqrt[3]{X_c} = K \text{ (eq. 2)}$$

In this equation, K is a constant equal to 0.24 for a variety of different hydroxyapatite powders, and B_{002} is FWHM (◦) of the (002) line.

The FTIR spectroscopy (Perkin Elmer Spectrum2, Singapore) analysis, using the KBr method, was performed in the 400–4000 cm^{-1} range with a scan speed of 23 scan/min at a 4 cm^{-1} resolution.

Formulation and characterization of experimental dental composites

The resin matrix was constructed by blending bisphenol A glycidyl methacrylate (Bis-GMA), triethylene glycol dimethacrylate (TEGDMA), and Hydroxyethyl methacrylate (HEMA) at a weight ratio of 2:1:1. Camphorquinone (0.1% w) and ethyl-4-dimethylamino benzoate (0.1% w) was included as a photo-initiator and co-initiator. All materials were obtained from Exir GmbH (Wien, Austria). We ensured a homogeneous mixture by stirring the resins with a magnetic stirrer in a dark beaker. Fillers were introduced at a weight ratio of 40% w/w and dispersed with a mechanical blender equipped with a Teflon head for 24 hours in a dark area. Accordingly, three types of resin-base composites were prepared including FHA250, FHA500, and FHA1000, which were filled with FHA fillers calcined at 250°C, 500°C, and 1000°C, respectively.

Three-point bending test

For evaluating flexural strength (FS) and modulus (FM), ten bar-shaped specimens of each composite, as well as the unfilled matrix resin, were prepared using a silicone mold. These specimens were shaped with dimensions of 2×2×25 mm. They were polymerized by a Bluephase LED light curing unit (Ivoclar Vivadent) employing a strategy of irradiating three overlapping regions, with each region receiving 40 seconds of exposure. After that, the silicone mold was carefully removed, and the back surface of each specimen was photo-polymerized to ensure complete polymerization. The specimens were

then stored in distilled water at a maintained temperature of 37°C for 24 hours. Then, a three-point bending method was employed in a universal testing machine (STM20, SANTAM, Iran) to evaluate the FS and FM of the specimens. The crosshead speed of the machine was set at 0.5 mm/min. The force experienced by the specimens at the point of fracture was utilized to calculate FS and FM according to the following formula:

$$F.S = \frac{3Fl}{2bh^2} \text{ (eq. 3-1)} \qquad F.M = \frac{l^3F}{4bh^3d} \text{ (eq. 3-2)}$$

In these equations, F represents the force at fracture, l indicates the distance between the supports (20 mm), b and h correspond to the width (2 mm) and height (2 mm) of the specimen, and d signifies the deflection due to the applied load (F) at the midpoint of the beam. Descriptive statistics, including mean and standard deviation values for FS and FM, were then calculated for each group.

Diametral tensile strength (DTS)

For each composite and the unfilled matrix resin, ten cylindrical specimens (height: 6 mm, diameter: 4 mm) were created. After fabrication, these specimens were stored in distilled water at 37°C for 24 hours. Subsequently, a compressive force at a rate of 0.5 mm/min was applied to the lateral surface of each specimen until fracture occurred. The force at the point of fracture was utilized to calculate the DTS according to the following formula:

$$DTS = \frac{2F}{\pi DH} \text{ (eq. 4)}$$

In this equation, F represents the force at fracture, H is the height of the cylinder (6 mm), and D is its diameter (4 mm).

To assess the effect of aging in an acidic environment, additional cylindrical specimens were created and stored in 10 mL of diluted acetic acid (pH=4.3) for 30 days. Following this period, the DTS of each specimen was measured. Mean DTS values for each group were calculated and compared with the mean DTS of samples that had not undergone the storage process.

Depth of cure evaluation

To assess the depth of cure, five cylindrical specimens (6 mm in height and 4 mm in diameter) were fabricated for each group and subsequently stored in distilled water at a controlled temperature of 37°C for 24 hours. After storage, the specimens were meticulously embedded within an acrylic resin matrix and sectioned longitudinally by a low-speed micro-saw under water cooling. Each sectioned specimen was then polished to produce a mirror-like surface. After that, the specimens were affixed onto the specimen stage of a Vickers microhardness (VMH) tester (Micro MH4, Koopa, Iran). The hardness was measured from the photo-cured surface down to a depth of 4 mm at increments of 0.5 mm. A total of three measurements were obtained for each depth, from which an average value was computed and reported as the VMH number. The relative VMH percentage was calculated via the following equation:

$$VMH\% \; at \; depth \; of \; x = \frac{VMH_0 - VMH_x}{VMH_0} \times 100$$

In this formula, VMH0 represents the VMH number at the surface. The depth of cure was eventually determined to be the depth at which the VMH% reached 80, as demonstrated in previous studies (23, 24).

Ion release evaluation

To measure the bioactivity of the composites, an analysis of the cumulative release of calcium and fluoride ions was carried out over one month. Five cylindrical specimens of each composite were prepared. Before photopolymerization, a thread was embedded in each composite to facilitate its subsequent suspension within the storage medium. The specimens were then placed within plastic tubes containing a diluted acetic acid solution (pH=4.3) and sealed before being stored at a constant temperature of 37°C. The specimens were cleaned with 5 cc of deionized distilled water at intervals of 1 and 24 hours, one week, and one month - before being transferred to a fresh storage medium. Fluoride ion was quantified using a fluoride ion selective electrode. For this purpose, 5cc of the combined solution was buffered using an equal volume of a total ionic strength adjustment buffer. Calcium ion concentration in the release media was determined using a Milton Roy Spectronic 20D spectrophotometer. The cumulative ion release from each specimen was then calculated in $\mu g/cm^2$ units.

Scanning Electron Microscopy (SEM)

The dispersion and the integrity of filler particles to the resin matrix were investigated using SEM (Leo 1450VP, Zeiss, Germany). For sample preparation, bar-shaped polymerized specimens were immersed in liquid nitrogen and fractured to create a clean surface. The fresh surface was gold sputtered and moved into the SEM chamber.

Statistical analysis

The normality of the data distribution was examined using the Kolmogorov-Smirnov Test. Then, one-way ANOVA was employed for the three-point bending test

to assess the impact of FHA fillers on FS and FM, followed by Tukey's test for multiple comparisons. Similarly, the effect of calcination temperature and storage in acidic media on the DTS was analyzed using two-way ANOVA. This led to the implementation of additional one-way ANOVA and Tukey's multi-comparison tests pre and post-storage, as well as independent samples t-tests for each calcination temperature. Furthermore, the depth of cure was determined by analyzing the profile of VMH% for each composite. The data analysis was performed through SPSS software (version 16.0; SPSS Inc, Chicago, Il, USA), and the significance level was determined at $P<0.05$.

Results

The characterization of synthesized fillers via XRD revealed a composite of phosphate-deficient hydroxyapatite (HA) and fluorapatite (FA) (Figure 1).

At lower calcination temperatures, the presence of phases and unconverted rhombohedral calcium phosphate were evident; however, these phases gradually diminished as the calcination temperature increased (Figure 1 and Table 1). As anticipated, a rise in calcination temperature corresponded to an increase in crystallinity percentage (Table 1), leading to more pronounced and well-defined apatite structural peaks.

The application of FTIR spectroscopy corroborated the formation of the apatite structure. Spectral bands located at specific wavenumbers corresponded to various bonds integral to the apatite structure (Figure 2). After citric acid treatment, new peaks emerged at 1594 cm-1 that were indicative of the reaction between citric acid and the surface of fillers. Additionally, the distortion of a peak in the FHA spectrum suggested the presence of a C-OH bond in the citrate structure.

The effects of FHA fillers on the flexural properties of the composites were evaluated using a three-point bending test and the results were significant ($P<0.05$; Table 2). Relative to the unfilled resin, the FS decreased with the addition of FHA250 fillers but remained almost unchanged for the FHA500 composite. Conversely, the FS for the FHA1000 composite exhibited a notable increase ($P<0.05$; Table 2). Regardless of the calcination temperature, the incorporation of FHA fillers significantly enhanced the FM ($P<0.05$; Table 2).

The DTS test results (Table 3) mirrored those of FS, with DTS decreased in the FHA250 composite compared to the unfilled resin. DTS was found to increase at calcination temperatures of 500°C, and 1000°C, and it significantly decreased after-acidic storage in all composites ($P<0.05$; Table 3).

In terms of curing depth (Figure 3), FHA1000 failed to reach the acceptable VMH% of 80 at a depth of 2 mm according to ISO4049 standards (24). Upon examining ion release, both calcium and fluoride ions initially exhibited rapid release followed by a steadier phase. Notably, calcium release practically ceased after the first week, whereas fluoride release continued at a steady rate for up to 30 days, and the release quantity was inversely proportional to the calcination temperature (Figure 4). Finally, SEM provided insights into the dispersion of FHA fillers in the three composites. Each composite displayed a different arrangement and size of particles, indicating the effect of calcination temperature on filler characteristics and distribution (Figure 5).

Table 1. Composition and distribution of phases detected by X-ray diffraction after Rietveld refinement. The percentages of crystalline phases are estimated.

Detected phases	Calcination temperature (ºC)		
	250	500	1000
HA (96-900-3549)	0.2%	47.4%	41.9%
FA (96-9001233)	47.2%	47.9%	58.1%
CHA (96-900-3553)	43.3%	2.3%	-
CFHA (96-900-9979)	9.2%	2.6%	-
Crystallinity (%)	48%	70%	95%

HA: hydroxyapatite; FA: Fluorapatite; CHA: Carbonated hydroxyapatite; CFHA: Carbonated Fluorohydroxyapatite

Table 2. Flexural strength (FS) and flexural modulus (FM) of unfilled resin-matrix and the experimental FHA-filled composites

Groups	FS Mean ± SD*	FM Mean ± SD*
Unfilled	31.44 ± 1.67 [b]	341.04 ± 32.55 [a]
FHA250	25.23 ± 3.55 [a]	996.20 ± 71.20 [b]
FHA500	31.15 ± 2.49 [b]	1095.20 ± 22.30 [c]
FHA1000	51.61 ± 6.25 [c]	1551.81 ± 63.17 [d]
P-value	0.004	<0.001

*Different letters indicate statistically significant differences at $P<0.05$.; SD: Standard deviation

Table 3. Diametral tensile strength (DTS) of the unfilled resin and the experimental FHA-filled composites before and after acidic storage

Groups	Without storage Mean ± SD*	With storage Mean ± SD*	% of DTS reduction	*P*-value
Unfilled	27.74 ± 4.21 [b]	15.47 ± 1.94 [a]	44.2%	<0.001
FHA250	21.48 ± 5.97 [a]	14.53 ± 1.75 [a]	32.4%	0.025
FHA500	30.22 ± 2.97 [b,c]	16.67 ± 2.57 [a]	44.8%	<0.001
FHA1000	35.72 ± 3.21 [c]	20.39 ± 1.34 [b]	54.2%	<0.001
P-value	<0.001	0.002		

*Different letters indicate statistically significant differences at P<0.05.; SD: Standard deviation

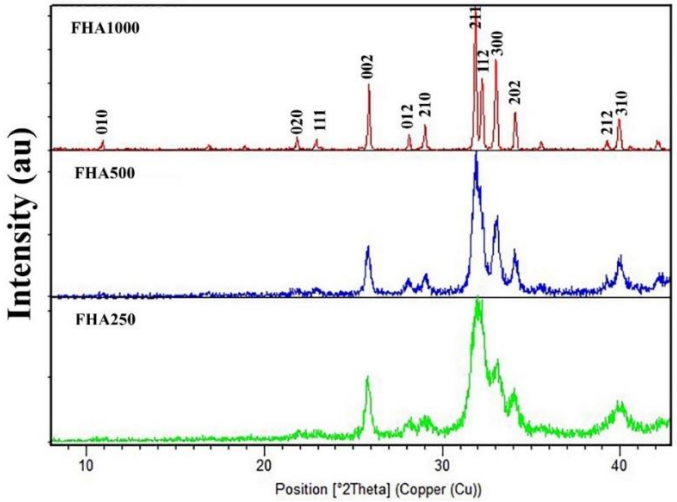

Figure 1. X-ray diffraction pattern of synthesized ceramic, calcined in three different temperatures. Numbers 250, 500, and 1000 show the temperature at which the fluorohydroxyapatite (FHA) was sintered.

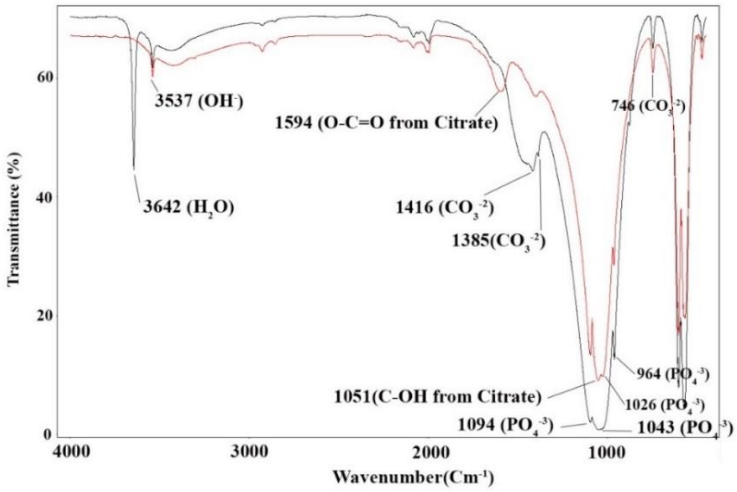

Figure 2. Fourier Transform Infrared spectrum of synthesized FHA500 and citric acid-modified FHA500

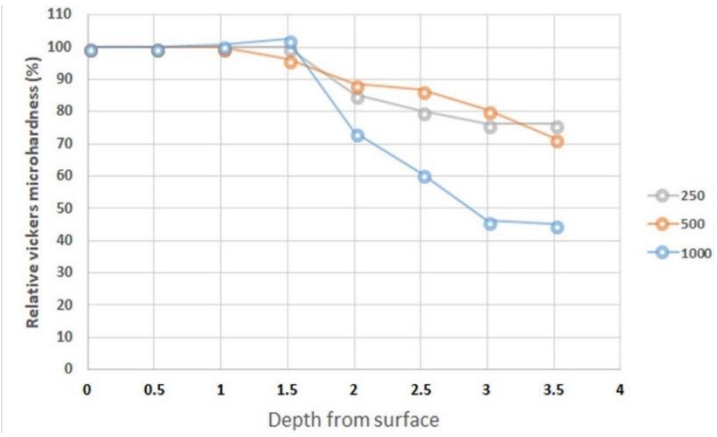

Figure 3. Profile of Vickers microhardness (VMH %) for three experimental composites.

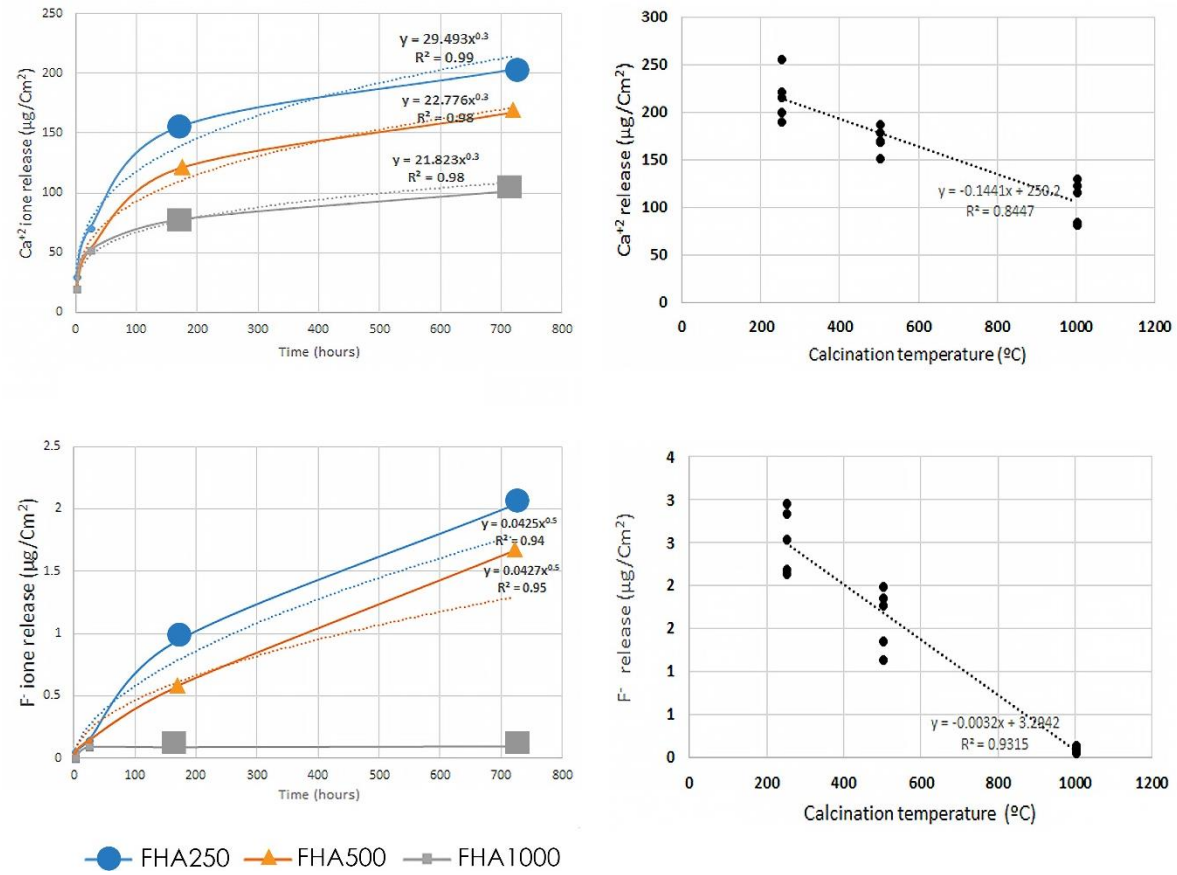

Figure 4. Calcium and fluoride ions release during the first month after polymerization in acidic media (pH=4.3). Linear regression analysis showed an indirect linear correlation between the calcination temperature and the amount of ion release.

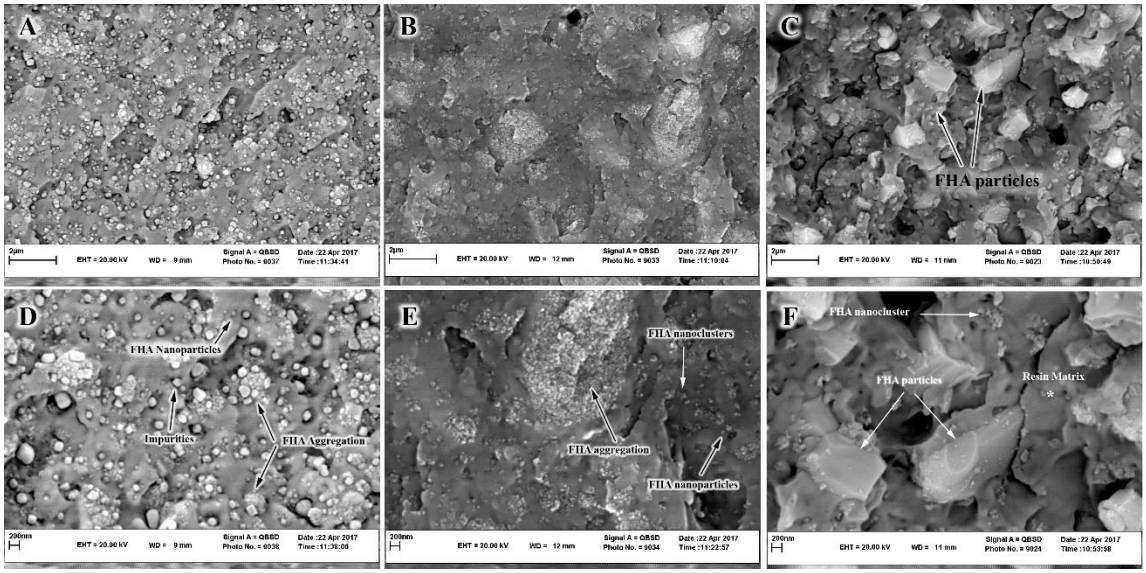

Figure 5. Scanning Electron Microscopy images for each composite, disclosing the distribution of FHA fillers (magnification: A to C: ×25,000; D to F: ×50,000). A&D: FHA250 composite, showing FHA nanoparticles and clusters. Impurities have not integrated with the resin matrix. B&E: FHA500 composite, with FHA nanoparticles and nanoclusters as well as aggregations, well integrated into the resin matrix. C&F: FHA1000 composite, high crystalline micron, and submicron fillers are indicated. Nanoclusters and aggregations are not seen as frequent as former samples.

Discussion

The performance characteristics of dental composites are greatly influenced by variables such as the resin matrix, filler type and distribution, and the quality of the resin-filler bond (25). In this study, we examined the impact of calcination temperature on the mechanical and physical properties, as well as the ion release of FHA-filled composites.

Characterization of the synthesized bioceramic validated the formation of calcium apatite phases, including HA,

FA, carbonated-hydroxyapatite (cHA), and carbonated-fluorapatite (CFA). Phosphate deficiency, which is attributed to the molar ratio of the reactants, can be compensated by fluoride or carbonate ions. The creation of carbonated phases can be related to the interaction of atmospheric carbon dioxide, which diminishes with increasing calcination temperature (26). Therefore, the present study demonstrates that calcination temperature significantly influences the microstructure and phase composition of synthetic bioceramics. This finding aligns with previous studies, showing increased crystallinity with rising temperature (21, 27).

Previous studies have investigated hydroxyapatite as a filler in dental composites (8, 9, 11, 14, 28). The results of this study are parallel to those of previous experiments (8, 9, 24, 29), highlighting the reinforcing impact of apatite fillers on dental composites. This study also reveals that the advantages of FHA fillers are influenced by the calcination temperature, a factor that in turn, has implications for the mechanical properties of the composite (30).

Several reasons could explain the observed effect of calcination temperature on composite strength. First, as previously noted, a higher calcination temperature results in a higher crystalline percentage of fillers (21, 22), leading to increased FS and DTS. Second, SEM evaluations indicated less agglomeration of nanoparticles in the FHA1000 composite (Figure 5 C and F). Previous studies have shown that filler agglomeration can create stress concentration points, affecting stress distribution, and resulting in brittle failure (24, 30, 31).

Despite the benefits of higher calcination temperatures, this study revealed a decrease in ion release with increasing the calcination temperature. This pattern can be attributed to an increase in the degree of crystallinity, reducing the fraction of more soluble phases (HA, cHA, and CFA) and consequently limiting ion release. Nevertheless, distinct patterns were discernible for calcium and fluoride ions (32).

Considering the dissolution of apatite fillers in acidic conditions, the impact of acidic storage on DTS was evaluated in this study. The data revealed a significant decrease in DTS after one month of acidic storage across all groups. This suggests that although DTS is influenced by the defects created by the dissolution of fillers, the softening of the resin matrix and the hydrolysis of the coupling agent have a more pronounced effect on DTS (33, 34). The FHA1000 composite exhibited a high degree of opacity, and its depth of cure was less than the ISO standard of 2 mm. These findings suggest that the high crystallinity of fillers obstructs light passage through the composite, potentially limiting the acceptable calcination temperature of FHA fillers.

This study had certain limitations that need to be considered when interpreting the results. Although the experimental setup allowed for a controlled study of individual components, it was unable to fully mimic the complexities of the oral environment. Future research could incorporate an in-vivo model to validate our findings under more realistic conditions, which will help to further refine the optimal conditions for the synthesis of FHA fillers. This study focused on the mechanical properties and ion release of FHA-filled composites. Future investigations could look at other important properties, such as thermal conductivity, color stability, and wear resistance, which are significant factors in the longevity and aesthetics of dental restorations. More studies are suggested to find out the optimum conditions for the synthesis of FHA fillers to be used in the formulation of smart dental composites.

Conclusions

Higher calcination temperature leads to greater crystalline apatite structure, which increases the mechanical properties but decreases ion release. Based on the mechanical and physical properties investigated in this study, it seems that FHA fillers, sintered around 500ºC may be suitable for formulation of a smart dental resin composite.

Conflict of Interest

The authors report no conflict of interest.

Acknowledgments

This research presents the results of the post-graduate thesis of the first author and was supported by grant no. 960125 from the Vice-Chancellor for Research and Technology, Mashhad University of Medical Sciences.

References

1. Moura FRRd, Romano AR, Lund RG, Piva E, Rodrigues Júnior SA, Demarco FF. Three-year clinical performance of composite restorations placed by undergraduate dental students. Braz Dent J 2011;22(2):111-116.

2. Opdam NJM, Sande FHvd, Bronkhorst E, Cenci MS, Bottenberg P, Pallesen U, et al. Longevity of Posterior Composite Restorations:A Systematic Review and Meta-analysis. J Dent Res 2014;93(10):943-949.

3. Shah YR, Shiraguppi VL, Deosarkar BA, Shelke UR. Long-term survival and reasons for failure in

direct anterior composite restorations: A systematic review. J Conserv Dent 2021;24(5):415-420.

4. De las Heras Alarcón C, Pennadam S, Alexander C. Stimuli-responsiv polymers for biomedical applications. Chem Soc Rev 2005;34(3):276-285.

5. Boskey AL, Posner AS. Conversion of amorphous calcium phosphate to microcrystalline hydroxyapatite. A pH-dependent, solution-mediated, solid-solid conversion. J Phys Chem 1973;77(19):2313-2317.

6. Bin-Jardan LI, Almadani DI, Almutairi LS, Almoabid HA, Alessa MA, Almulhim KS, et al. Inorganic Compounds as Remineralizing Fillers in Dental Restorative Materials: Narrative Review. Int J Mol Sci 2023;24(9).

7. Ren J, Rao J, Wang H, He W, Feng J, Wei D, et al. Synergistic remineralization of enamel white spot lesions using mesoporous bioactive glasses loaded with amorphous calcium phosphate. Front Bioeng Biotechnol 2023;11.

8. Labella R, Braden M, Deb S. Novel hydroxyapatite-based dental composites. Biomaterials 1994;15(15):1197-200.

9. Arcís RW, López-Macipe A, Toledano M, Osorio E, Rodríguez-Clemente R, Murtra J, et al. Mechanical properties of visible light-cured resins reinforced with hydroxyapatite for dental restoration. Dent Mater 2002;18(1):49-57.

10. Santos C, Clarke R, Braden M, Guitian F, Davy K. Water absorption characteristics of dental composites incorporating hydroxyapatite filler. Biomaterials 2002;23(8):1897-1904.

11. Ai M, Du Z, Zhu S, Geng H, Zhang X, Cai Q, et al. Composite resin reinforced with silver nanoparticles–laden hydroxyapatite nanowires for dental application. Dent Mater 2017;33(1):12-22.

12. Rodrigues MC, Xavier TA, Arana-Chavez VE, Braga RR. Polymer-based material containing calcium phosphate particles functionalized with a dimethacrylate monomer for use in restorative dentistry. J Biomater Appli 2017;31(6):871-877.

13. Al-Hamdan RS, Almutairi B, Kattan HF, Alsuwailem NA, Farooq I, Vohra F, et al. Influence of hydroxyapatite nanospheres in dentin adhesive on the dentin bond integrity and degree of conversion: A Scanning Electron Microscopy (SEM), Raman, Fourier Transform-Infrared (FTIR), and microtensile study. Polymers 2020;12(12).

14. Jardim RN, Rocha AA, Rossi AM, de Almeida Neves A, Portela MB, Lopes RT, et al. Fabrication and characterization of remineralizing dental composites containing hydroxyapatite nanoparticles. J Mech Behav Biomed Mater 2020;109.

15. Wu Y-R, Chang C-W, Ko C-L, Wu H-Y, Chen W-C. The morphological effect of calcium phosphates as reinforcement in methacrylate-based dental composite resins on mechanical strength through thermal cycling. Ceram Int 2017;43(16):14389-14394.

16. Behroozibakhsh M, Shafiei F, Hooshmand T, Moztarzadeh F, Tahriri M, Gorgani HB. Effect of a synthetic nanocrystalline-fluorohydroxyapatite on the eroded enamel lesions. Dent Mater 2014;2014(30):e117-e118.

17. Wang Q, Liu S, Gao X, Wei Y, Deng X, Chen H, et al. Remineralizing efficacy of fluorohydroxyapatite gel on artificial dentinal caries lesion. J Nanomater 2015;2015

18. Lin J, Zhu J, Gu X, Wen W, Li Q, Fischer-Brandies H, et al. Effects of incorporation of nano-fluorapatite or nano-fluorohydroxyapatite on a resin-modified glass ionomer cement. Acta Biomaterialia. 2011;7(3):1346-1353.

19. Gualandi P, Gualandi A, Gualandi J, Foltran I, Foresti E, Lelli M, et al. Dental care products comprising carbonate-substituted fluoro-hydroxyapatite particles. Pat USA 2016.

20. Chaiwat A, Chunhacheevachaloke E, Kidkhunthod P, Pakawanit P, Ajcharanukul O. Enamel Remineralization and Crystallization after Fluoride Iontophoresis. J Dent Res 2023;102(4):402-411.

21. Garskaite E, Gross K-A, Yang S-W, Yang TC-K, Yang J-C, Kareiva A. Effect of processing conditions on the crystallinity and structure of carbonated calcium hydroxyapatite (CHAp). Cryst Eng Comm 2014;16(19):3950-3959.

22. Sanosh K, Chu M-C, Balakrishnan A, Kim T, Cho S-J. Preparation and characterization of nano-hydroxyapatite powder using sol-gel technique. Bull Mater Sci 2009;32(5):465-470.

23. Corr, #xea, a JM, Mori M, Sanches H, #xed, et al. Silver Nanoparticles in Dental Biomaterials. Int J Biomater 2015;2015.

24. Shyang CW, Khim LY, Ariffin A, Arifin Z, Ishak M. Flexural properties of hydroxyapatite reinforced poly (methyl methacrylate) composites. J Reinf Plast Compos 2008;27(9):945-952.

25. Ferracane JL. Resin composite—state of the art. Dental Materials 2011;27(1):29-38.

26. Ślósarczyk A, Paszkiewicz Z, Paluszkiewicz C. FTIR and XRD evaluation of carbonated hydroxyapatite powders synthesized by wet methods. J Mol Struct 2005;744:657-661.

27. Edie D. The effect of processing on the structure and properties of carbon fibers. Carbon 1998;36(4):345-362.

28. Domingo C, Arcís R, López-Macipe A, Osorio R, Rodríguez-Clemente R, Murtra J, et al. Dental composites reinforced with hydroxyapatite: mechanical behavior and absorption/elution characteristics. J Biomed Mater Res 2001;56(2):297-305.

29. Santos C, Luklinska Z, Clarke R, Davy K. Hydroxyapatite as a filler for dental composite materials: mechanical properties and in vitro bioactivity of composites. J Mater Sci Mater Med 2001;12(7):565-573.

30. Zhang H, Darvell BW. Mechanical properties of hydroxyapatite whisker-reinforced bis-GMA-based resin composites. Dent Mater 2012;28(8):824-830.

31. Curtis AR, Palin WM, Fleming GJ, Shortall AC, Marquis PM. The mechanical properties of nanofilled resin-based composites: characterizing discrete filler particles and agglomerates using a micromanipulation technique. Dent Mater 2009;25(2):180-187.

32. Xu X, Burgess JO. Compressive strength, fluoride release and recharge of fluoride-releasing materials. Biomaterials 2003;24(14):2451-461.

33. De Moraes RR, Marimon JLM, Jochims Schneider LF, Sinhoreti MAC, Correr-Sobrinho L, Bueno M. Effects of 6 months of aging in water on hardness and surface roughness of two microhybrid dental composites. J Prosthodont 2008;17(4):323-326.

34. Ghavami-Lahiji M, Firouzmanesh M, Bagheri H, Jafarzadeh Kashi TS, Razazpour F, Behroozibakhsh M. The effect of thermocycling on the degree of conversion and mechanical properties of a microhybrid dental resin composite. Restor Dent Endod 2018;43(2).

35. Asmussen E, Peutzfeldt A. Long-term fluoride release from a glass ionomer cement, a compomer, and from experimental resin composites. Acta Odontol Scand 2002;60(2):93-97.